Punjab University
Journal of Mathematics (ISSN 1016-2526)
Vol. 51(4)(2019) pp. 13-36

Bioconvection Model for Magneto Hydrodynamics Squeezing Nanofluid Flow with Heat and Mass Transfer Between Two Parallel Plates Containing Gyrotactic Microorganisms Under the Influence of Thermal Radiations

Syed Asif Hussain[1,2], Gohar Ali[1], Syed Inayat Ali Shah[1], Sher Muhammad[1,2,*], Mohammad Ishaq[1]

[1]Department of Mathematics, Islamia College, Peshawar 25000, Khyber Pakhtunkhwa, Pakistan.

[2]Cecos University of IT and Emerging Sciences Peshawar 25000, Khyber Pakhtunkhwa, Pakistan.

* Corresponding author : Sher Muhammad
Email: (shermuhammad@cecos.edu.pk)

Received: 06 April, 2018 / Accepted: 16 July, 2018 / Published online: 03 January, 2019

Abstract. This research paper investigates the bioconvection magneto hydrodynamics (MHD) squeezing nanofluid flow between two parallel plates. One of the plates is stretched and the other is kept fixed. In this study the water is taken as a base fluid because it is a favorable fluid for living microorganisms. Appropriate variables lead to a strong nonlinear ordinary differential system. The obtained nonlinear system has been solved via homotopy analysis method (HAM). The significant influences of thermophoresis and Brownian motion have also been taken in nanofluid model. The convergence of the method has been shown numerically. The variation of the Skin friction, Nusselt number, Sherwood number and their effects on the velocity, concentration, temperature and the density motile microorganism profiles are examined. It is observed that increasing thermal radiation augmented the temperature of the boundary layer area in fluid layer. This increase leads to drop in the rate of cooling for nanofluid flow. An interesting variation are inspected for the density of the motile microorganisms due to the varying bioconvection parameter in suction and injection cases. Furthermore, for comprehension the physical presentation of the embedded parameters, such as unsteady squeezing parameter (λ) , Thermal radiation parameter (Rd), Peclet number (Pe), Thermophoresis parameter (Nt), Levis number (Le) , Prandtl number (Pr), Schmidt number (Sc)and Brownian motion parameter (Nb) are plotted and discussed graphically. At the end, we made some concluding remarks in the light of this research article.

Key Words: MHD, Squeezing flow, Nano fluid, Parallel plates, Gyrotactic Microorganisms and HAM.

1. INTRODUCTION

Bioconvection model for MHD squeezing flow with heat and mass transfer between two parallel plates containing gyrotactic microorganisms under the influence of thermal radiation has been studied. It plays a very important role in the real world phenomena and has vast applications which attract the researchers. Squeezing flow between the parallel plates has received the attention of recent researchers due to widespread significance in different fields, particularly in mechanical engineering, chemical engineering and food industry etc. (see [12, 23]). Many scientists worked in this field, according to their levels and needs. A number of publications are available to explain and demonstrate the properties and behaviour of squeezing nanofluid for industrial applications like nuclear reactions, foods, electronics, biomechanics, transportations etc. There are several examples regarding squeezing flow, important are injection, compression and polymer preparation. This field got considerable attention due to useful applications in the Biophysical and Physical field as well. Stefan [51] has been explored squeezing flow using lubrication approximation. Verma [52] has studied squeezing flow between parallel plates. Singh et al. [49] highlighted mass relocation and the effect of thermophoresis and Brownian motion. Acharya et al. [4] investigated flow of the Cu water and Cu-kerosene nanofluid between parallel plates. Hayat et al. [20] explored magneto-hydrodynamic (MHD) effect on squeezing flow in Jeffery nanofluids for parallel disc.Heat transfer plays a very important role in industrial and practical situations. In many practical and industrial situations, heat exchanged in the system with the help of fluid. Heat transfer has plenty of useful applications in many equipment's such as heat exchangers, thermal conductivity and the heat transfer coefficient of the fluid which have a significant role. In order to improve the heat transfer efficiency different researchers have been investigated heat transfer in the nanofluids [13,17,29,42,45]. In the light of the growing world competition in many industries and the role of heat transfer in the costs of production, researchers turned their attention towards the new class of fluids that have more effective thermal properties as compared to that of regular fluids. This sort of fluids are suspended in the base fluid uninterruptedly and stably. Water, glycol and kerosene oil, etc. are used as the base fluids. For thermal conductivity of the nanofluid, several models have been proposed. For instance, we can study [13,29] and references therein. Firstly, Choi [13] explored the concept of enhancing thermal conductivity of the base fluid (water, glycol and kerosene oil, etc.). They termed such type of fluid as nanofluid. Nano-fluid is the composition of Nano-particles, which shows significant properties at a reticent concentration of Nano-particles. Nano-fluid is a term refers to liquid consisting sub micro particles. It has abundant applications, but the important feature is the development of thermal conductivity observed by Masuda et al. [39]. Her investigation reveals that Nano-fluid has different thermal properties like thermal viscosity, thermal infeasibility, and relocation of temperature, convection temperature and thermal conductivity as compared to oil and water base fluids [14,15,16,53]. Hamad [18] has been investigated the Nano-fluid analytical solution for convection flow in occurrence of magnetic field. Flow of nanofluid between parallel plates is one of the benchmark problems which have important and crucial applications. Goodman [19] was the first one to investigate viscous fluid in parallel plates. Borkakoti and Bharali [10] have been investigated Hydro magnetic viscous flow between parallel plates where one of the plates is a stretching sheet. Sheikholeslami et al. [8,47,48] studied nanofluid flow of viscous fluids between parallel plates with rotating systems in three dimensions under the magneto hydrodynamics (MHD) effects. Mahmoodi and Kandelousi [38] have examined the hydro magnetic effect of Kerosene?alumina nanofluid flow in the occurrence of heat transfer analysis, differential transformation method is used in their work. Thermal radiation is also a part of this investigation and has an important role in flow phenomena. It has various applications because of its dependence on temperature difference, as the polymer processing industries are using the radiation effects for the transformation of heat. The common ways of transfer of heat in industry is not beneficial nowadays. The radiations play significant role in heat transfer. Hayat et al. [21] discussed thermal radiations influence in squeezing flows of Jeffery fluids. Ali et al. [6] investigated effect of radiations on unsteady free convection magneto hydrodynamics flows of the Brinkman kind fluids in a porous medium have Newtonian heat. The flow of mass by temperature gradient named Sort effects or thermal diffusion and energy flows due to mass flow by temperature gradient is known Dufour effect or diffusion thermal effect and it is reciprocal of the first one. Thermal diffusion is used for separation of different isotopes of medium and light molecular weight. Nakhi and Chamkha [11] have been investigated MHD mixed radiation- convection interaction of permeable surface absorbed at porous medium being there of Sorts and Dufours effect. Srinivasacharya [50] has been investigated both the effects in vertical curly surface in the existence of the porous medium. One of the very significant motive regarding the heat transfer enhancements in the nanofluid is the addition of microorganisms. The addition of microorganisms (bacteria and algae) in the base fluid elaborates the operation of bioconvection. [43] Which is preceded by their up-spinning oxygen, gravity and the source of light and their density tends to be slightly greater as compared to the ambient fluid and leads to an unstable density field. The dilution of microorganisms in the nanofluids amends its thermal conductivity importantly. The mixed convection flow of the nanoparticles and microorganisms is called gyrotactic microorganisms. Recently, Khan et al. [30] and Ammarah et al. [44] explored the problem of the bioconvection flow in different geometries. Khan et al [26] studied magnetic and Navier slip effect in heat and mass transfer in gyrotactic micro-organism in vertical surface. Similarly, Khan with Makinde [27] have been studied boundary layer flow of MHD in Nano-fluid consisting gyrotactic organism in linearly stretching sheet. In the present field of science and engineering most of mathematical problems are so complex in their nature that the accurate solution is almost extremely difficult. So for the solution of such problems, Numerical and Analytical methods are used to find the approximate solution. One of the important and popular techniques for solution of such type problems is HAM (Homotopy Analysis Method) [1,2,32,33,34,37] and the recent work about analytical solution and HAM can also be seen in [3,5,7,9,22,24,25,28,31,40,41,46,54]. Homotopy analysis Method is a substitute method and its main advantage is applying to the nonlinear differential equations without discretization and linearization.In this manuscript, we study the bioconvection flow of a nanofluid between two parallel plates in the presence of microorganisms under the influence of thermal radiation. Water is taken as a base fluid for the survival of the microorganisms. The Well-known Homotopy analysis Method is utilized for numerical and analytical solutions, respectively. The influence of all nondimensional physical parameters embedded in the bioconvection flow model is studied graphically as a function of velocity, temperature, concentration and density of the motile microorganisms for suction and injection, respectively. Many similar and improved results have been found and discussed analytically with the help of various graphs. The problem is formulated in section 2 and transformed into the dimensionless system of ordinary differential equations that describes the bioconvection flow between parallel plates. The next section presents problem development. Section 3 depicts the development of convergent series solutions. Analysis for convergence and discussion have been examined in Sections 4 and 5, respectively. Section 6 gives the main outcomes of the present study.

2. Problem's Mathematical Formulation:

The calculations and modelling used in this research article are explained as: The unsteady, two-dimensional and symmetric-nature flow of a viscous incompressible fluid between two parallel plates with the effects of MHD and thermal radiations is considered. The plates are placed in the Cartesian coordinates system in such a way that the lower plate is on the horizontal x-axis, and the y-axis is at the perpendicular position to the lower plate and the lower plate is fixed. It is assumed that the distance between these parallel plates is y = h, where h is a function of t. Furthermore, it is assumed that the lower plate is capable of moving away or towards the lower plate placed at y = 0. This plate (upper Plate) moves with $v(t) = \frac{dh}{dt}$ and the constant magnetic-field B_0 is acting in the y-direction. The temperatures at the upper and lower plates are T_1 and T_2, respectively. It is also assumed that both plates (upper and lower) are maintained at constant temperature. Where upper plate has reflexive supporting conditions and nanoparticles are scattered uniformly at lower plate. Uniform microorganisms distribution on the upper plate represented by N_2 and lower plate by N_1 . The nanoparticles are scattered uniformly on the lower plate. The geometry of the nanofluid flow phenomena is shown in Fig.1.

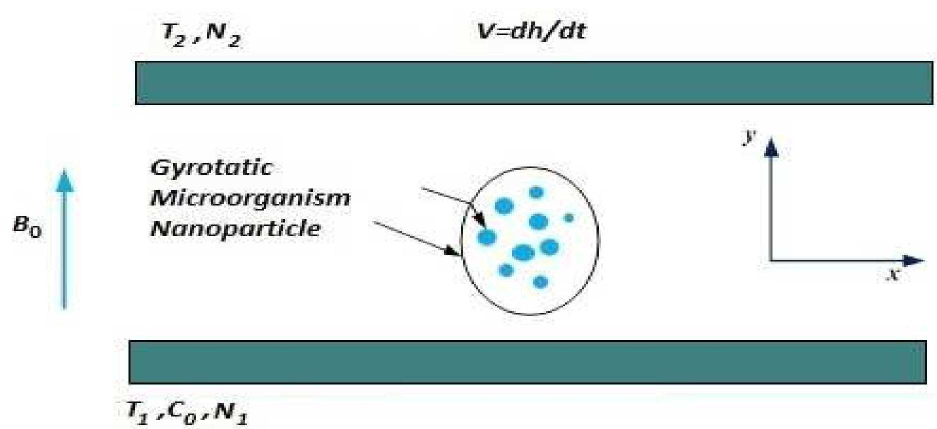

FIGURE 1. Geometry of the Nanofluid flow.

Observance in the above deliberation, the elementary equations are continuity, velocity, heat, concentration and density of the motile microorganism are articulated [9] as follows,

$$\frac{\partial \widehat{u}}{\partial x}+\frac{\partial \widehat{v}}{\partial y}=0, \tag{2. 1}$$

$$\rho\left[\frac{\partial \widehat{u}}{\partial t}+\widehat{u}\frac{\partial \widehat{u}}{\partial x}+\widehat{v}\frac{\partial \widehat{u}}{\partial y}\right]=-\frac{\partial p}{\partial x}+\mu\left(\frac{\partial^2 \widehat{u}}{\partial x^2}+\frac{\partial^2 \widehat{v}}{\partial y^2}\right)-\sigma B_0^2\widehat{u}(t), \tag{2. 2}$$

$$\rho\left[\frac{\partial \widehat{v}}{\partial t}+\widehat{u}\frac{\partial \widehat{v}}{\partial x}+\widehat{v}\frac{\partial \widehat{v}}{\partial y}\right]=-\frac{\partial p}{\partial y}+\mu\left(\frac{\partial^2 \widehat{v}}{\partial x^2}+\frac{\partial^2 \widehat{v}}{\partial y^2}\right), \tag{2. 3}$$

$$\frac{\partial T}{\partial t}+\widehat{u}\frac{\partial T}{\partial x}+\widehat{v}\frac{\partial T}{\partial y}=\widehat{\alpha}\left(\frac{\partial^2 T}{\partial x^2}+\frac{\partial^2 T}{\partial y^2}\right)+\tau\begin{bmatrix} D_B\left(\frac{\partial C}{\partial x}\frac{\partial T}{\partial x}+\frac{\partial C}{\partial y}\frac{\partial T}{\partial y}\right)+ \\ \frac{D_T}{T_0}\left[(\frac{\partial T}{\partial x})^2+(\frac{\partial T}{\partial y})^2\right]\end{bmatrix} -\frac{1}{(\rho c_p)_f}\frac{\partial q_{rd}}{\partial y}, \tag{2. 4}$$

$$\frac{\partial C}{\partial t}+\widehat{u}\frac{\partial C}{\partial x}+\widehat{v}\frac{\partial C}{\partial y}=D_B\left(\frac{\partial^2 C}{\partial x^2}+\frac{\partial^2 C}{\partial y^2}\right)\frac{D_T}{T_0}\left[\frac{\partial^2 T}{\partial x^2}+\frac{\partial^2 T}{\partial y^2}\right], \tag{2. 5}$$

$$\frac{\partial N}{\partial t}+\widehat{u}\frac{\partial N}{\partial x}+\widehat{v}\frac{\partial N}{\partial y}+\frac{\partial (Nv*)}{\partial z}=D_n\frac{\partial^2 N}{\partial y^2}, \tag{2. 6}$$

In above mentioned Eqs. (2.1 - 2.6) $\widehat{u}$ and $\widehat{v}$ denotes velocity components, T and C represents the temperature at the plate and the volumetric fraction of the nanoparticles, N be density of the motile-microorganism, $\tau=\frac{(\rho c)_p}{(\rho c)_f}$, where $(\rho c)_p$ and $(\rho c)_f$ represents temperature capacity of nanoparticles and fluids. Moreover, μ denotes viscosity, D_B represents Brownian diffusion and D_T denotes thermophoretic coefficient, in x and y directions respectively. Eqs. (2.1 - 2.6) represents the flow model for nanofluid. Further $v^*=\frac{bw_c}{\Delta C}\frac{\partial C}{\partial y}$. In Eq (2.4), q_{rd} is the radiative heat fluctuation is expressed in term of Roseland approximation as:

$$q_{rd}=-\frac{4\sigma^*}{3K^*}\frac{\partial T^4}{\partial y}, \tag{2. 7}$$

where in the above equation (2.7) K^* and σ^* denoted the mean absorption coefficient and the Stefan Boltzmann constant respectively. Supposing that the difference in heat inside the flow is such that T^4 can be expressed as a linear-combination of the heat, we enlarge T^4 as a Taylor's series about as under:

$$T^4=T_0^4+4T_0^3\left(T-T_0\right)^2+... \tag{2. 8}$$

After ignoring terms of higher order term, we obtain:

$$T^4=4TT_0^3-3T_0^4. \tag{2. 9}$$

By Putting Eq. (2.8) in Eq. (2.7) we get

$$\frac{\partial q_r}{\partial y}=-\frac{16\sigma^* T_0^3}{3K^*}\frac{\partial^2 T}{\partial y^2}. \tag{2. 10}$$

For lower and upper plates feasible auxiliary conditions are:

$$\widehat{u} = 0, \quad \widehat{v} = 0, \quad T = T_1, \quad C = C_1, \quad N = N_1, \tag{2. 11}$$

$$\widehat{v} = \frac{dh}{dx}, \quad \widehat{u} = 0, \quad T = T_2, \quad D_B(\frac{\partial C}{\partial y}) + \frac{D_T}{T_0}(\frac{\partial T}{\partial y}) = 0, \quad N = N_2, \tag{2. 12}$$

For the flow model of microorganism the non-dimensional similarity variables are:

$$\Psi(x,y) = \left(\tfrac{1-\alpha t}{bv}\right)^{\frac{-1}{2}} xf(\eta), u = \left(\tfrac{1-\alpha t}{bx}\right)^{-1} f'(\eta), v = -\left(\tfrac{1-\alpha t}{bv}\right)^{\frac{-1}{2}} f(\eta), \tag{2. 13}$$
$$\eta = \left(\tfrac{v(1-\alpha t)}{b}\right)^{\frac{-1}{2}} y, \theta(\eta) = \left(\tfrac{T-T_0}{T_2-T_0}\right), \phi(\eta) = -1 + \frac{C}{C_0}, and\theta(\eta) = \left(\tfrac{N-N_0}{N_2-N_0}\right),$$

Substituting Eq. (2.13) into the governing Eqs. (2.1-2.6), we develop the subsequent succeeding transformed ODE's that are given bellow:

$$f^{iv} + ff''' - f'f'' - \lambda\eta f''' - 3\lambda f'' - Mf'' = 0, \tag{2. 14}$$

$$\left(1 + \tfrac{4}{3}\right)\theta'' + Pr(f - \lambda\eta)\theta' + Nb\phi'\theta' + Nt(\theta')^2 = 0, \tag{2. 15}$$

$$\phi'' + Le(f - \lambda\eta)\phi' + \left(\tfrac{Nt}{Nb}\right)\theta'' = 0, \tag{2. 16}$$

$$\varphi'' + Sc(f - \lambda\eta)\varphi' + Pe\varphi\phi'' - Pe\varphi'\phi' = 0. \tag{2. 17}$$

The non-dimensional parameters after simplification are written as:

(2. 18)
$$\lambda = \frac{\alpha}{2b}, M = \frac{\sigma B_0^2}{\rho b}(1-\alpha t), Rd = \frac{4T^3\sigma}{3(\rho c_p)_f k\alpha}, Sc = \frac{v}{D_n}, Nt = \frac{(\rho c)_p}{(\rho c)_f}\frac{D_T(T_2 - T_0)}{T_0\alpha},$$
$$Nb = \frac{(\rho c)_p}{(\rho c)_f}\frac{D_b C_0}{\alpha}, Pr = \frac{v}{\alpha}, Pe = \frac{b_c W_c}{D_n}, Le = \frac{v}{D_B}, \omega = \frac{\alpha H}{2(vb)^{\frac{1}{2}}}, \delta\varphi = \frac{N_1 - N_0}{N_2 - N_0},$$
$$\delta\phi = \frac{C_1 - C_0}{C_0}, \delta\theta = \frac{T_1 - T_0}{T_2 - T_0}$$

In the above model equations (2.14 - 2.17) unlike parameters are used like λ represent unsteady squeezing parameter, The other dimensionless physical parameter which are used in the Flow Model are thermal radiation (Rd) , Peclet number (Pe), Levis number (Le) , Brownian motion (Nb), Prandtl number (Pr), Schmidt number (Sc) and thermophoresis parameter (Nt). Also ω, δ_ϕ, δ_φ, and δ_θ all are constants. Furthermore, transmuted form of the feasible boundary conditions both for lower as well as for upper plates defined in equations (2.11) and (2.12) are as:

$$f(0) = 0, f'(0) = 0, f'(1) = 0, f(1) = w, \theta(1) = \delta_\theta, \theta(0) = 1, \tag{2. 19}$$
$$\phi(1) = \delta_\phi, \varphi(1) = \delta_\varphi, \phi(0)Nb + \theta'(0)Nt = 0, \varphi(0) = 1.$$

The Skin-Friction, Nusselt Number, Sherwood Number and the Density Number of the motile microorganism are defined under as:

(2. 20)
$$C_f = \frac{2\tau\omega}{\rho U_w^2}, Nu_x = \frac{xq_w}{K(T_w - T_0)}, Sh_x = \frac{xq_m}{D_B(C_w - C_0)}, Nn_x = \frac{xq_n}{D_n(n_w - n_0)},$$
$$\tau_\omega = |\mu\frac{\partial u}{\partial y}|_{y=0}, q_\omega = |K\frac{\partial T}{\partial y}|_{y=0}, q_m = | - D_B\frac{\partial \phi}{\partial y}|_{y=0}, q_n = | - D_n\frac{\partial \zeta}{\partial y}|_{y=0},$$

By using Eq. (2.13) dimensionless form, Nusselt Number, Skin-Friction, Sherwood Number and Local-Density of motile microorganisms are as:

(2. 21)
$$\frac{\sqrt{Re_x}}{2}C_f = f''(0), Nu_x(Re_x)^{-1/2} = -\theta'(0), Sh_x(Re_x)^{-1/2} = -\phi'(0),$$
$$and\, Nn_x(Re_x)^{-1/2} = -\zeta'(0).$$

Where $Re_x = \frac{xU_\omega}{v}$ is signifies a local Reynolds number.

3. SOLUTION BY HAM:

In order to solve Eqs. (2.14 - 2.17) with boundary-conditions (2.19), we apply "Homotopy Analysis Method". For the solution HAM scheme has advantage such as it is free from large or small parameters. This technique offers an easy way to confirm convergence of the solution. Moreover, it delivers freedom for the right selection of auxiliary parameters and base function. In this scheme the assisting parameter $\hbar$ is used to control the convergence of the problem The initial guesses and linear operators for the dimensionless momentum, energy, concentration and density of motile microorganism equations are $(f_0, \theta_0, \phi_0, \varphi_0)$ and $(L_f, L_\theta, L_\phi, L_\varphi)$ These are presented in the forms:

(3. 22)
$$f_0(\eta) = 3\omega\eta^2 - 2\eta^3, \theta_0(\eta) = 1 - \eta + \delta_\theta\eta, \varphi_0(\eta) = 1 - \eta + \delta_\varphi\eta,$$
$$\phi_0(\eta) = \frac{1}{Nb}(-Nt + Nt\eta + Nt\delta_\theta - Nt\delta_\theta\eta + Nb\delta_\phi).$$

Selected linear operators, are:

(3. 23)
$$L_f(f) = \frac{\partial^4 f}{\partial\eta^4}, L_\theta(\theta) = \frac{\partial^2\theta}{\partial\eta^2}, L_\phi(\phi) = \frac{\partial^2\phi}{\partial\eta^2}, L_\varphi(\varphi) = \frac{\partial^2\varphi}{\partial\eta^2}.$$

The above mentioned differential operators contents are shown below:

(3. 24)
$$L_f(\epsilon_1 + \epsilon_2\eta + \epsilon_3\eta^2) + \epsilon_4\eta^3) = 0, L_\theta(\epsilon_5 + \epsilon_6\eta) = 0, L_\phi(\epsilon_7 + \epsilon_8\eta) = 0,$$
$$L_\varphi(\epsilon_9 + \epsilon_{10}\eta) = 0.$$

Here $\sum_{i=1}^{10}\epsilon_i$ where $i = 1, 2, 3, ...$ denotes arbitrary constants. The resultant non-linear operators are given by: N_f,N_θ,N_ϕ, and N_φ.

(3. 25)
$$N_f\left[\widehat{f}(\eta;\xi)\right] = \frac{\partial^4\widehat{f}(\eta;\xi)}{\partial\eta^4} + \widehat{f}(\eta;\xi)\frac{\partial^2\widehat{f}(\eta;\xi)}{\partial\eta^2} - \frac{\partial\widehat{f}(\eta;\xi)}{\partial\eta}\frac{\partial^2\widehat{f}(\eta;\xi)}{\partial\eta^2}$$
$$- \lambda\eta\frac{\partial^3\widehat{f}(\eta;\xi)}{\partial\eta^3} - 3\lambda\frac{\partial^2\widehat{f}(\eta;\xi)}{\partial\eta^2} - M\frac{\partial^2\widehat{f}(\eta;\xi)}{\partial\eta^2}$$

$$N_\theta\left[\widehat{f}(\eta;\xi),\widehat{\theta}(\eta;\xi),\widehat{\phi}(\eta;\xi)\right]=\left(1+\tfrac{4}{3}Rd\right)\frac{\partial^2\widehat{\theta}(\eta;\xi)}{\partial\eta^2}+Pr(f(\eta;\xi)-\lambda\eta)\frac{\partial\widehat{\theta}(\eta;\xi)}{\partial\eta}+Nb\frac{\partial\widehat{\theta}(\eta;\xi)}{\partial\eta}\frac{\partial\widehat{\phi}(\eta;\xi)}{\partial\eta}+Nt\left(\tfrac{\partial\widehat{\theta}(\eta;\xi)}{\partial\eta}\right)^2 \tag{3. 26}$$

$$N_\phi\left[\widehat{f}(\eta;\xi),\widehat{\theta}(\eta;\xi),\widehat{\phi}(\eta;\xi)\right]=\frac{\partial^2\widehat{\phi}}{\partial\eta^2}+Le(f(\eta;\xi)-\lambda\eta)\frac{\partial\widehat{\phi}(\eta;\xi)}{\partial\eta}+\frac{Nt}{Nb}\frac{\partial^2\widehat{\theta}(\eta;\xi)}{\partial\eta^2} \tag{3. 27}$$

$$N_\varphi\left[\widehat{f}(\eta;\xi),\widehat{\varphi}(\eta;\xi),\widehat{\phi}(\eta;\xi)\right]=\frac{\partial^2\widehat{\varphi}}{\partial\eta^2}+Sc(f(\eta;\xi)-\lambda\eta)\frac{\partial\widehat{\varphi}(\eta;\xi)}{\partial\eta}-Pe\widehat{\varphi}(\eta;\xi)\frac{\partial^2\widehat{\varphi}}{\partial\eta^2}-Pe\frac{\partial\widehat{\phi}}{\partial\eta}\frac{\partial\widehat{\varphi}}{\partial\eta} \tag{3. 28}$$

4. Zeroth Order Deformation Problem:

$$(1-\xi)L_f[\widehat{f}(\eta,\xi)-\widehat{f}_0(\eta)]=\psi h_f N_f[\widehat{f}(\eta,\xi)] \tag{4. 29}$$

$$(1-\xi)L_\theta[\widehat{\theta}(\eta,\xi)-\widehat{\theta}_0(\eta)]=\xi h_\theta N_\theta[\widehat{f}(\eta,\xi),\widehat{\theta}(\eta,\xi),\widehat{\phi}(\eta,\xi)] \tag{4. 30}$$

$$(1-\xi)L_\phi[\widehat{\phi}(\eta,\xi)-\widehat{\phi}_0(\eta)]=\xi h_\phi N_\phi[\widehat{f}(\eta,\xi),\widehat{\theta}(\eta,\xi),\widehat{\phi}(\eta,\xi)] \tag{4. 31}$$

$$(1-\xi)L_\varphi[\widehat{\varphi}(\eta,\xi)-\widehat{\varphi}_0(\eta)]=\xi h_\varphi N_\varphi[\widehat{f}(\eta,\xi),\widehat{\theta}(\eta,\xi),\widehat{\varphi}(\eta,\xi)] \tag{4. 32}$$

The subjected boundary conditions are derived as:

$$\widehat{f}(\eta,\xi)|_{\eta=0}=0,\qquad \widehat{f}(\eta,\xi)|_{\eta=1}=w, \tag{4. 33}$$

$$\widehat{\theta}(\eta,\xi)|_{\eta=0}=1,\qquad \widehat{f}(\eta,\xi)|_{\eta=1}=\delta_\theta, \tag{4. 34}$$

$$\widehat{\varphi}(\eta,\xi)|_{\eta=0}=1,\qquad \widehat{\varphi}(\eta,\xi)|_{\eta=1}=\delta_\varphi, \tag{4. 35}$$

$$\frac{\partial\widehat{f}(\eta,\xi)}{\partial\eta}|_{\eta=0}=0,\qquad \frac{\partial\widehat{f}(\eta,\xi)}{\partial\eta}|_{\eta=1}=0, \tag{4. 36}$$

$$\widehat{\phi}(\eta,\xi)|_{\eta=1}=\delta_\phi,\qquad Nb\widehat{\phi}(\eta,\xi)|_{\eta=0}+Nt\frac{\partial\widehat{\theta}(\eta,\xi)}{\partial\eta}|_{\eta=0}=0, \tag{4. 37}$$

where $\xi\in[0,1]$ is the embedding constraint, h_f, h_θ, h_ϕ, h_φ were used to regulate convergence of the solution. Where $\xi=0$, $\xi=1$ we have;

$$\widehat{f}(\eta)=\widehat{f}(\eta,1),\qquad \widehat{\theta}(\eta)=\widehat{\theta}(\eta,1),\qquad \widehat{\phi}(\eta)=\widehat{\phi}(\eta,1),\qquad \widehat{\varphi}(\eta)=\widehat{\varphi}(\eta,1) \tag{4. 38}$$

Expanding the above term of ξ with use of Taylor's series expansion we obtain:

$$\widehat{f}(\eta,\xi)=\widehat{f}_0(\eta)+\sum_{i=1}^{\infty}\widehat{f}_i(\eta) \tag{4. 39}$$

$$\widehat{\theta}(\eta,\xi)=\widehat{\theta}_0(\eta)+\sum_{i=1}^{\infty}\widehat{\theta}_i(\eta) \tag{4. 40}$$

$$\widehat{\phi}(\eta,\xi)=\widehat{\phi}_0(\eta)+\sum_{i=1}^{\infty}\widehat{\phi}_i(\eta) \tag{4. 41}$$

$$\widehat{\varphi}(\eta,\xi)=\widehat{\varphi}_0(\eta)+\sum_{i=1}^{\infty}\widehat{\varphi}_i(\eta) \tag{4. 42}$$

$$\widehat{f}_i(\eta)=\frac{1}{i!}\frac{\partial\widehat{f}(\eta,\xi)}{\partial\eta}\mid_{\eta=0},\qquad \widehat{\theta}_i(\eta)=\frac{1}{i!}\frac{\partial\widehat{\theta}(\eta,\xi)}{\partial\eta}\mid_{\eta=0},$$
$$\widehat{\phi}_i(\eta)=\frac{1}{i!}\frac{\partial\widehat{\phi}(\eta,\xi)}{\partial\eta}\mid_{\eta=0},\qquad \widehat{\varphi}_i(\eta)=\frac{1}{i!}\frac{\partial\widehat{\varphi}(\eta,\xi)}{\partial\eta}\mid_{\eta=0} \tag{4. 43}$$

5. I^{th} Order Deformation Problem:

Differentiating Zeroth Order equations i^{th} times we obtained the i^{th} Order deformation equations with respect to ξ dividing by $i!$ and then inserting $\xi=0$ So, i^{th} order deformation equations are:

$$L_f\left[\widehat{f}_i(\eta)-\zeta_i\widehat{f}_{i-1}(\eta)\right]=h_fR_i^f(\eta), \tag{5. 44}$$

$$L_\theta\left[\widehat{\theta}_{ii}(\eta)-\zeta_i\widehat{\theta}_{i-1}(\eta)\right]=h_\theta R_i^\theta(\eta), \tag{5. 45}$$

$$L_\phi\left[\widehat{\phi}_i(\eta)-\zeta_i\widehat{\phi}_{i-1}(\eta)\right]=h_\phi R_i^\phi(\eta). \tag{5. 46}$$

$$L_\varphi\left[\widehat{\varphi}_i(\eta)-\zeta_i\widehat{\varphi}_{i-1}(\eta)\right]=h_\varphi R_i^\varphi(\eta). \tag{5. 47}$$

The resulting boundary conditions are:

$$\widehat{f}_i(0)=\widehat{f}_i'(0)=\widehat{\theta}_{ii}(0)=\widehat{\phi}_i(1)=\widehat{f}_i(1)=\widehat{f}_i'(1)=\widehat{\theta}_{ii}(1)$$
$$=\widehat{\varphi}_{ii}(0)=\widehat{\varphi}_{ii}(1)=0, Nb\widehat{\phi}_i(0)+Nt\widehat{\theta}_i'(0)=0 \tag{5. 48}$$

and

$$R_i^f(\eta) = \widehat{f}_{i-1}^{iv} + \sum_{k=0}^{i-1} \widehat{f}_{i-1-k}\widehat{f}_k''' + \sum_{k=0}^{i-1} \widehat{f}'_{i-1-k}\widehat{f}''_k - \lambda\eta\widehat{f}'''_{i-1} - 3\lambda\widehat{f}''_{i-1} - M\widehat{f}''_{i-1}, \tag{5. 49}$$

$$R_i^\theta(\eta) = \left(1 + \tfrac{4}{3}Rd\right)\widehat{\theta}''_{i-1} + Pr\left(\textstyle\sum_{k=0}^{i-1} \widehat{f}_{i-1-k}\widehat{\theta}'_k - \lambda\eta\widehat{\theta}'_{i-1}\right) + Nb\sum_{k=0}^{i-1} \widehat{\phi}'_{i-1-k}\widehat{\theta}'_k + Nt\sum_{k=0}^{i-1} \widehat{\theta}'_{i-1-k}\widehat{\theta}'_k \tag{5. 50}$$

$$R_i^\phi(\eta) = \widehat{\phi}''_{i-1} + Le\left(\textstyle\sum_{k=0}^{i-1} \widehat{f}_{i-1-k}\widehat{\phi}'_k - \lambda\eta\widehat{\phi}'_{i-1}\right) + \frac{Nt}{Nb}\widehat{\theta}''_{i-1}, \tag{5. 51}$$

$$R_i^\varphi(\eta) = \widehat{\varphi}''_{i-1} + Sc\left(\textstyle\sum_{k=0}^{i-1} \widehat{f}_{i-1-k}\widehat{\varphi}'_k - \lambda\eta\widehat{\varphi}'_{i-1}\right) + Pe\sum_{k=0}^{i-1} \widehat{\varphi}'_{i-1-k}\widehat{\phi}''_k - Pe\sum_{k=0}^{i-1} \widehat{\varphi}'_{i-1-k}\widehat{\phi}'_k, \tag{5. 52}$$

Where

$$\zeta_i = \begin{cases} 1, & \xi > 1 \\ 0, & \xi \leqslant 1 \end{cases} \tag{5. 53}$$

6. CONVERGENCE:

When the series solutions is calculated for the velocity, density of motile microorganism, temperature and concentration functions via using HAM, the assisting parameters are h_f,h_θ,h_ϕ and h_φ. These main parameters are responsible for the convergence of the solution. To get the possible region of the h-Curves graph of $f''(0)$,$\theta'(0)$,$\varphi'(0)$ and $\phi'(0)$ for 13^{th} order approximation are plotted in the Figures. (1-2). The h-curves consecutively display the valid region. In HAM technique the convergence region is important to determine the meaningful series solutions of the governing problems of $f''(0)$,$\theta'(0)$,$\varphi'(0)$ and $\phi'(0)$. The parameters h_f,h_θ, h_ϕ and h_φ are employed to control solution. Moreover, the h-curves are plotted at 13^{th} order approximation. From the h-curves we observed the appropriate ranges for h_f,h_θ,h_ϕ and h_φ are $-2.3 \leq h_f \leq 0.2$, $-2.2 \leq h_\theta \leq 0.1$, $-2.5 \leq h_\phi \leq 0.5$, and $-2.1 \leq h_\varphi \leq 0.4$.

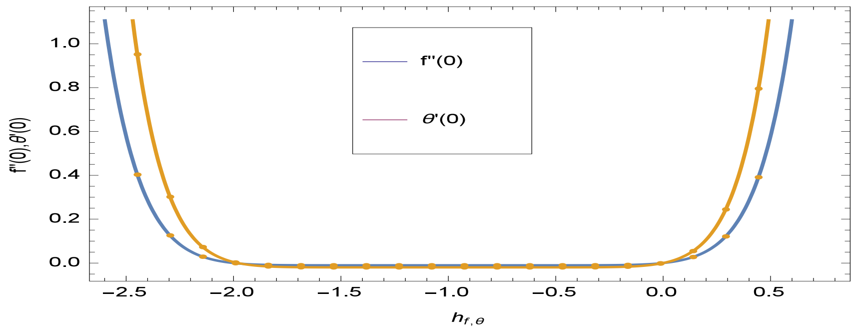

FIGURE 2. The combined curve of functions at 13^{th} order approximation.

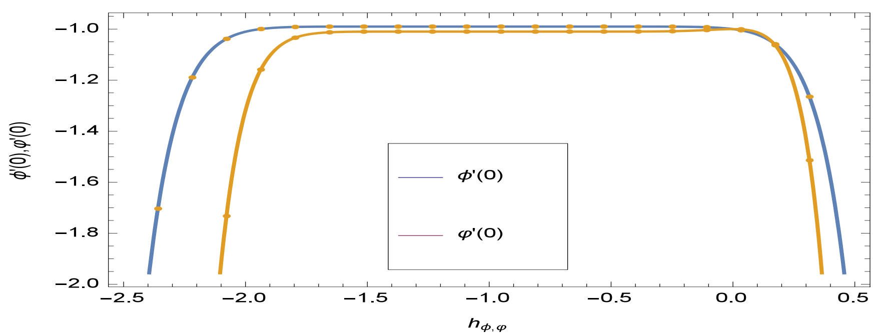

FIGURE 3. The combined curve of functions and at 13^{th} order approximation.

Table 1.Represents convergence of the HAM up to 13^{th} Order Approximation where, $\lambda = M = Nt = 0.5$,$Pr = 0.7$,$Nb = 1$,$Le = 0.6$,$Sc = 0.8$,$\omega = Rd = 0.1$,$Pe = 0.7$.

Approximation Order	$f''(0)$	$\theta'(0)$	$\phi'(0)$	$\varphi'(0)$
1	3.98886	-0.0207921	0.953750	1.00025
3	3.97650	-0.0387064	0.913169	1.07375
5	3.97584	-0.0396453	0.910490	1.08915
7	3.97583	-0.0396677	0.910384	1.09009
9	3.97583	-0.0396682	0.910379	1.09014
13	3.97583	-0.0396682	0.910379	1.09014

7. RESULT AND DISCUSSION:

In this portion we have disclosed the physical interpretation of sundry variables involving into the problem and is about to understand the effects of various non-dimensional physical quantities on the Velocity $f(\eta)$, Heat $\theta(\eta)$, Concentration $\phi(\eta)$ and Density of motile microorganism $\varphi(\eta)$ profiles. The following results with complete details are achieved: Fig. 1 shows geometry of the fluid model for comprehensions of the readers. The h-curves are elaborated in Figs. (2-3). Figs 4,5,6 and 7 represent the influences of squeezing fluid parameter λ on $f(\eta)$, $\theta(\eta)$, $\phi(\eta)$ and $\varphi(\eta)$. When plates are moving apart, then λ takes the positive value in that corresponding case and when plates are coming closer the values are considered negative. Figure.4 clearly shows the influence of the flow when plates are moving away and this is opposite case of when plates coming nearer. With the increase of λ values fluid velocity also increasing. Clearly velocity increases in the channel when fluid sucked inside. On the other hand when fluid injected out, then the plates come closer to one another. This manner brings about a drop in the fluid and consequently decreases the velocity. With varying value of λ parameter the influence of $f(\eta)$ shown in fig. 4. Figs. 5 and 6 show the influence of λ parameter on the heat and concentration distributions respectively. Due to squeezing of the fluid the velocity increases and subsequently falls the temperature of the fluid because warm nanoparticles are escaping rapidly which results in lower temperature and the concentration of the fluid automatically reduces. Fig.7 indicates variation in density of the motile microorganisms for various values of λ. The density of microorganisms $\varphi(\eta)$ illustrates variations. With changing λ values, the $\varphi(\eta)$ is a decreasing factor, when λ parameter changes negatively and it shows increasing function for positive values of λ. Fig.8 demonstrates the impact of velocity field for various values of magnetic field parameter M. It depicts that with an increase in value of M, velocity profile decreases, because Lorentz forces work against the flow and those regions where its influences dominates, it reduces velocity. After a certain distance it increases. Figs.9 demonstrates the characteristics of magnetic parameter M on heat distribution , which is increasing for higher values and drops for the small values of M. Actually Lorentz force decreasing which depend on magnetic field M, so decreasing M leads to decrease Lorentz force and consequently decreases $\theta(\eta)$. The impact of Pr on the $\theta(\eta)$ and $\phi(\eta)$ are shown in Figs. 10 and 11. Clearly it is seen that temperature and concentration distributions vary inversely with Pr, that is temperature distribution drop with large numbers of Pr and rise for lesser values of Pr. Physically, the fluids having a small number of Pr has larger thermal diffusivity and this effect is opposite for higher Prandtl number. Due to this fact large Pr causes the thermal boundary layer to decrease. The effect is even more diverse for the small number of Pr since thermal boundary layer thickness is relatively large. On the other hand increasing behaviour of concentration distribution is shown in fig.11 for increasing Pr values. Figs.12 represents the influence of thermophoretic parameter Nt on heat profile $\theta(\eta)$. It is investigated that $\theta(\eta)$ is increased by varying thermophoretic parameter Nt. According to Kinetic Molecular theory increasing number of particles and increasing number of active particles both can cause to increase in the heat factor. Fig.13 represents the change in the concentration profile $\phi(\eta)$ due to change in parameter Nt. The profile $\phi(\eta)$ decreases in suction and injection cases. In injection case, the decrement in $\phi(\eta)$ is slow as compare to fluid suction case. Figs.14 and15 show the effect of Nb on $\theta(\eta)$ and $\phi(\eta)$ fields.

Heat profile $\theta(\eta)$ is increased by varying values of Nb as shown in fig. 14. Due to Kinetic molecular theory the heat of the fluid increases due to the increase of Brownian motion. So the given result is in good agreement with real situation. Similarly fig.15 highlights the impact of varying Nb parameter with respect to the concentration profile $\phi(\eta)$ on domain, $0 \leq \lambda \leq 1$. An increasing impact of $\phi(\eta)$ is observed for both suction and injection in fig.15. A fast increment has been observed in $\phi(\eta)$ for fluid suction as compared to fluid injection. Fig.16 represents the effect of Peclet number Pe on $\varphi(\eta)$. The values of density field of motile microorganism increase with increase value of Pe. Fig. 17 shows the impacts of on density field of motile microorganism $\varphi(\eta)$.The values of density field of the motile microorganisms decrease with increase in the values of Sc. Actually, Schmidt number is the ratio of kinematic viscosity to the mass flux. So when kinematic viscosity increases, then spontaneously the Sc increases and $\varphi(\eta)$ decreases. Fig. 18 displays the influence of Le on the concentration profile $\phi(\eta)$ where it decreases when number Le increases. Actually, it is the ratio of thermal diffusivity to the mass diffusivity. So, when the thermal diffusivity decreases it automatically decreases Le and also decreases concentration field. Fig. 19 displays the effect of radiation parameter Rd on the heat field $\theta(\eta)$. It is clearly observed that heat profile $\theta(\eta)$ decreases with increase values of Rd. It is a common observation that radiating a fluid or some other thing can cause to reduce the temperature of that particular object.

8. TABLE DISCUSSIONS:

Table.1 displays numerical values of HAM solutions at different approximation using various values of different parameters. It is clear from the table.1 that homotopy analysis technique is a quickly convergent technique. Physical quantities such as skin friction co-efficient, heat flux, mass flux and Local-density number of motile microorganism for engineering interest are calculated through Tables: (2-5). Table: 2 displays the impact of inserting parameters M and λ on Skin friction C_f. It is seen that increasing value of M and λ decreases the skin friction C_f. Table.3 examines the influences of embedding parameters Nb,Nt,Pr and Rd on heat flux Nu. It is seen that increasing values of Pr increase the heat flux Nu where Rd,Nt and Nb decrease the heat flux when it increased. Table.4 inspects the influences of Le,Nb and Nt on mass flux Sh. The increasing values of Le and Nb increase the mass flux where Nt reduces the mass flux .The influences of Sc,λ and Pe on $\varphi'(0)$ are shown in Table.5. The increasing values of Pe increases $\varphi'(0)$, while the higher value of λ and Sc reduce $\varphi'(0)$.

Table 2. Represents numerical values of the Skin-Friction Co-efficient for various parameters where $Nb = 1$,$Nt = Le = 0.6$,$Sc = 0.8$,$Pe = 0.7$ and $\omega = 0.1$.

M	λ	$-(C_f Re_x)^{\frac{1}{2}}$ Hayat et al. [22] result	$-(C_f Re_x)^{\frac{1}{2}}$ Present Results
0.1	1.5	-2.40160	1.1051
0.5		-2.41735	0.9999
1.0		-2.42522	0.9957
0.1	1.5	-2.40788	1.2057
	2.0	-2.40828	1.1947
	2.5	-2.40947	1.1747
	3.0	-2.41426	0.9957

Table 3. Represents Numerical values of Local-Nusselt number for unlike type parameters, where $Pr = 0.7$,$\lambda = 1$,$Le = 0.6$,$Sc = 0.8$,$Pe = 0.7$,$\omega = 0.1$ and $M = 0.5$.

Rd	Nt	Nb	Pr	$-\theta'(0)$ Alsaedi el al [7].Results	$-\theta'(0)$ Present Result
0.5	0.5	0.5	1.0	.....	2.0003
0.1				.....	1.6202
1.5				.....	1.2133
0.5	0.5			0.8167	1.9501
	1.0			0.6971	1.5546
	1.5			0.5735	1.2013
	0.5			0.8943	2.5923
		0.5		0.8011	1.7456
		1.0	1.0	0.7472	1.0072
		0.5	1.5	0.8943	1.1196
			2.0	1.0270	17456

Table 4. Represents Numerical type values of Local-Sherwood number for unlike parameters, where $Le = 0.6$,$Sc = 0.8$,$Pe = Pr = 0.7$,$\omega = 0.1$,$\lambda = M = 0.6$.

Le	Nb	Nt	$-\phi'(0)$ Alsaedi el al [7].Results	$-\phi'(0)$ Present Result
0.1	0.2	0.5	0.4471	0.8518
0.5			0.5878	0.9618
1.0	0.2		0.5878	0.6624
	0.6		0.9582	0.7910
	1.0		1.0320	0.8518
	0.2	0.5	0.5878	0.8615
		1.0	0.8588	0.9020
		1.5	-0.3914	0.8901

Table 5. Represents Numerical values of Local-density number of motile microorganism for various types of parameters, when $Sc = 0.8$,$Pr = 1$,$Pe = 0.7$,$\omega = 0.1$,$\lambda = M = 0.5$.

Sc	λ	Pe	$-\varphi'(0)$ Alsaedi el al [7].Results	$-\varphi'(0)$ Present Result
1.0	0.5	0.5	.....	1.6434
1.5			.....	1.2526
2.0			.....	0.9542
1.0	0.5		.....	2.1053
	1.0		.....	1.8599
	1.5		.....	0.9552
	0.5	0.5	1.3811	1.6864
		1.5	1.4764	1.7801
		2.0	1.5731	2.1053

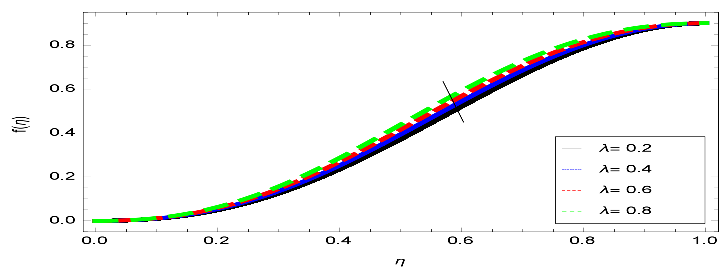

FIGURE 4. Effect of λ on $f(\eta)$, when $\omega = 0.8$ and $M = 1.9$.

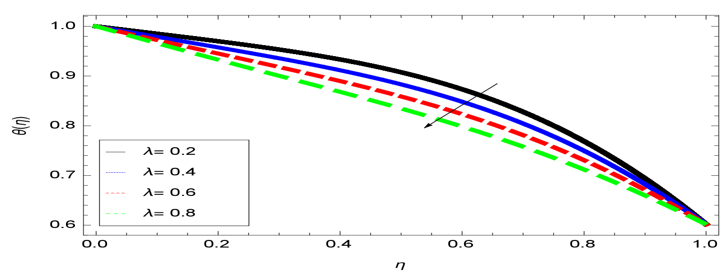

FIGURE 5. Effect of λ on $\theta(\eta)$, when $\omega = 0.8$,$Le = 0.4$,$Nt = 0.1$,$Nb = Rd = 0.4$,$Pr = 0.6$.

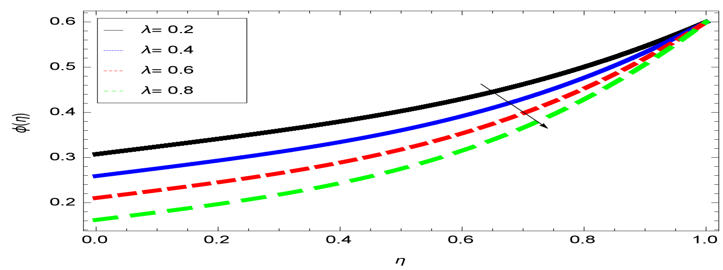

FIGURE 6. Effect of λ on $\phi(\eta)$, when $\omega = 0.8$,$Le = 0.4$,$Nt = 0.1$,$Nb = 0.6$,$Pr = 0.6$ and $M = 0.5$.

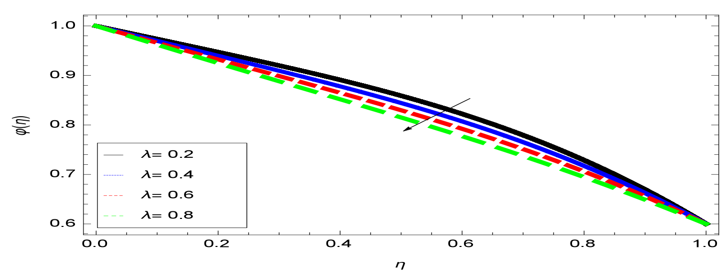

FIGURE 7. Effect of λ on $\varphi(\eta)$, when $\omega = 0.8$,$Le = Sc = 0.4$,$Nt = Pe = 0.1$,$Nb = 0.3$ and $M = 1$.

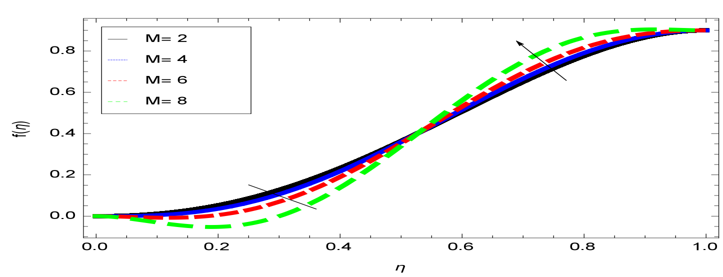

FIGURE 8. Effect of M on $f(\eta)$, when $\omega = 0.8$ and $\lambda = 0.9$.

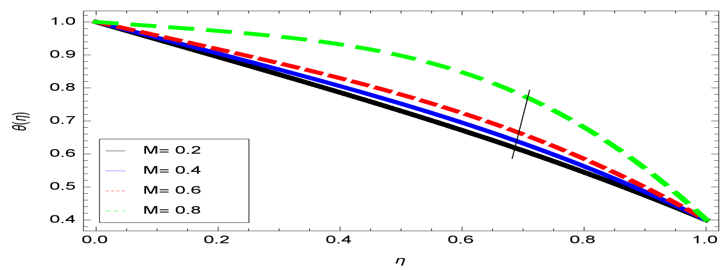

FIGURE 9. Effect of M on $\theta(\eta)$, when $\omega = 0.8$,$Le = 0.3$,$Nt = 0.6$,$Nb = 0.1$,$\lambda = Rd = 1$,$Pr = 0.5$.

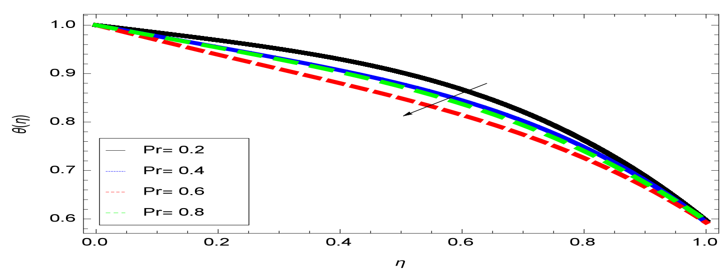

FIGURE 10. Effect of Pr on $\theta(\eta)$, when $\omega = 0.8$,$Le = 0.3$,$Nt = 0.6$,$\lambda = Rd = 0.4$,$Nb = 0.1$,$M = 1$.

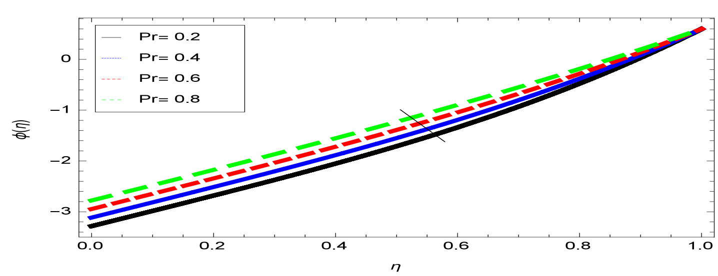

FIGURE 11. Effect of Pr on $\phi(\eta)$, when $\omega = 0.8$,$Le = 0.3$,$Nt = 0.6$,$\lambda = 0.4$,$Nb = 0.1$,$Pr = 0.2$,$M = 1$.

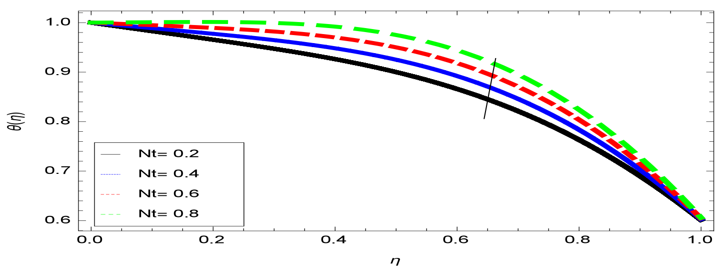

FIGURE 12. Effect of Nt on $\theta(\eta)$, when $\omega = 0.8$,$Le = 0.3$,$\lambda = Rd = 0.4$,$Nb = 0.1$,$Pr = 0.6$,$M = 2$.

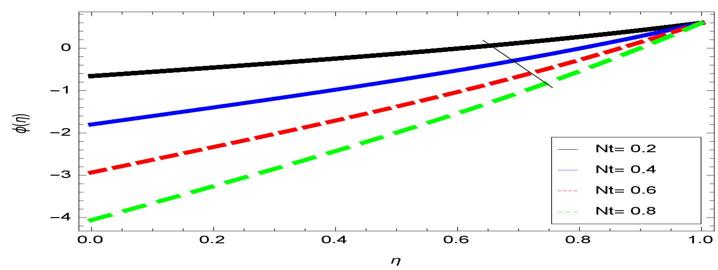

FIGURE 13. Effect of Nt on $\phi(\eta)$, when $\omega = 0.8$,$Le = 0.3$,$\lambda = 0.4$,$Nb = 0.1$,$Pr = 0.6$,$M = 2$.

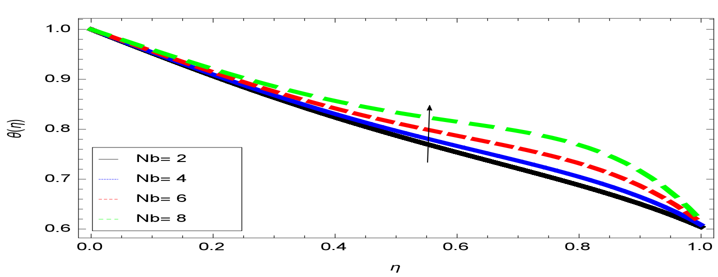

FIGURE 14. Effect of Nb on $\theta(\eta)$, when $\omega = 0.8$,$Le = 0.3$,$\lambda = Rd = 0.4$,$Nt = 0.1$,$Pr = 0.6$,$M = 2$.

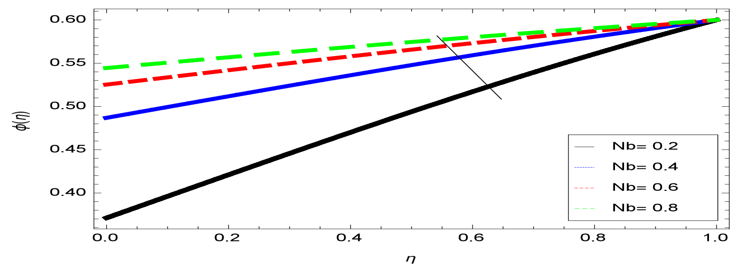

FIGURE 15. Effect of Nb on $\phi(\eta)$, when $\omega = 0.8$,$Le = 0.3$,$\lambda = 0.4$,$Nt = 0.1$,$Pr = 0.6$,$M = 1$.

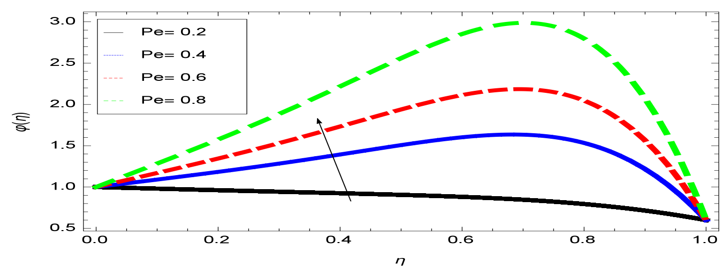

FIGURE 16. Effect of Pe on $\varphi(\eta)$, when $\omega = 0.8$,$Le = 0.3$,$\lambda = Sc = 0.4$,$Nb = 0.1$,$Nt = 0.6$,$M = 2$.

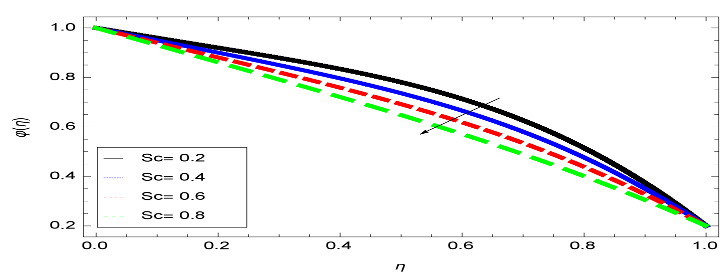

FIGURE 17. Effect of Sc on $\varphi(\eta)$, when $\omega = 0.8$,$Le = 0.3$,$\lambda = 0.4$,$Nb = 0.1$,$Nt = 0.6$,$Pr = 0.5$,$M = 1$.

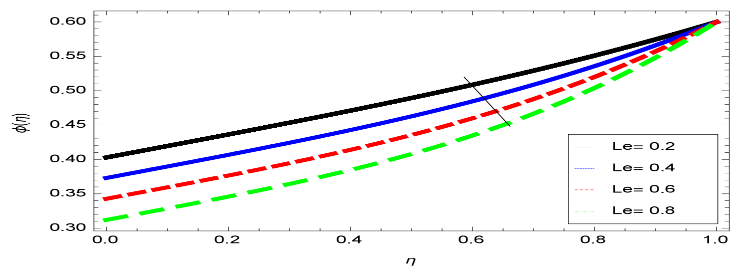

FIGURE 18. Effect of Le on $\phi(\eta)$, when $\omega = 0.8$,$Le = 0.4$,$\lambda = 4$,$Nt = 0.1$,$Nb = 0.3$,$Pr = 0.6$,$M = 1$.

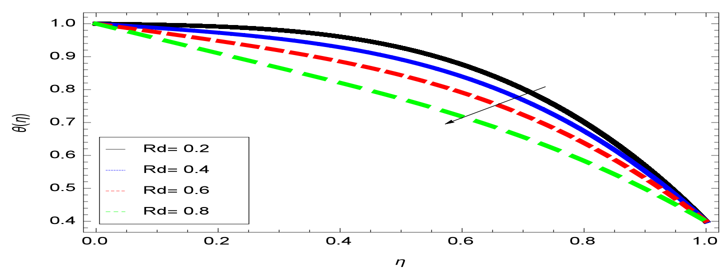

FIGURE 19. Effect of Rd on $\theta(\eta)$, when $\omega = Le = 0.8$,$\lambda = 4$,$Nb = 0.1$,$Nt = 0.6$,$Pr = 0.5$,$M = 1.9$.

9. CONCLUDING REMARKS:

In this research article, bioconvection flow between two parallel plates is under consideration. It is assumed that the plates are capable to expand or contract. The dimensional flow model included the nanofluid and microorganisms transformed into the nondimensional and highly nonlinear system of ordinary differential equations. For this, a defined dimensionless form of the similarity variables is utilized. Also, the supporting boundary conditions are reduced in dimensionless form.Effect of embedding parameters are observed and discussed graphically. Furthermore, the variation of the Skin friction, Sherwood number, Nusselt number and their effects on the velocity, concentration, temperature and motile microorganism profiles are examined. The key points are:

- The larger values of Nb rise the kinetic energy of the nanoparticles, which result an increase in the heat profile.
- When we increase thermal radiation parameter Rd, then it augments temperature of the boundary layer area in fluid layer. This increase leads to drop in the rate of cooling for nanofluid flow.

- It is observed that $\theta(\eta)$ is increased by varying thermophoretic parameter Nt.
- Thermophoretic and Brownian motion parameters affect the concentration field reversely for both the suction and injection case.
- The convergence of the homotopy method along with the variation of different physical parameters has been observed numerically.
- Interesting variations in the density of motile microorganisms φ are analyzed for different values of the bioconvection parameter.
- It is seen that increasing M and λ reduce the skin friction C_f.
- It is seen that increasing values of Pr increases the heat flux Nu while Nb, Nt and Rd reduce the heat flux Nu.
- The increasing values of Le and Nb increase the mass flux where Nt reduces the mass flux.
- For the suction/injection parameter λ, Brownian parameter Nb and thermophoretic parameter Nt the density of motile microorganisms shows very prominent variations throughout the domain of interest.

10. Nomenclature:

The following abbreviations are used in this manuscript:

B_0	Magnetic field strength
Rd	Rediation parameter
M	Magnetic parameter
D_B	Brownian diffusion of nanofluids
Nt	Thermophoretic parameter
Nb	Brownian motion parameter
Sh	Sherhood number
Nu	Nusslet number
Re	Reynold number
Pr	Prandtl number
Sc	Schmidth number
C_{ref}	Reference concentration
T_{ref}	Reference temperature
τ_{ij}	Extra stress tensor
ν	Kinematic viscosity
μ	Dynamic viscosity
T	Temperature
$\widehat{k}$	Thermal conductivity
q_{rd}	Radioactive heat fluctuation
σ^*	Stefan Boltzmann constant
k^*	Mean absorption coefficient
β	Film Thickness parameter
λ	Unsteady squeezing parameter
ρ	Density

11. Acknowledgement

The authors are highly grateful to Professor Dr. Gohar Ali and Professor Dr. Syed Inayat Ali Shah for his constructive comments, helpful remarks, encouragement and research advise from start to finish despite all odds.The authors are also thankful to the anonymous reviewers for their fruitful comments and to the Editor-in-Chief for his dedecation and active correspondance.

12. AUTHORCONTRIBUTIONS

Conceptualization: Syed Asif Hussain and Gohar Ali, Methodology: Syed Asif Hussain and Sher Muhammad, Software: Mohammad Ishaq and Sher Muhammad, Validation: Syed Asif Hussain, Gohar Ali, Syed Inayat Ali Shah and Mohammad Ishaq, Formal Analysis: Syed Asif Hussain,Mohammad Ishaq Investigation: Syed Asif Hussain,Sher Muhammad, Resources: Syed Asif Hussain, WritingOriginal Draft Preparation: Syed Asif Hussain, WritingReview & Editing: Mohammad Ishaq and Sher Muhammad, Visualization: Syed Inayat Ali Shah and Syed Asif Hussain, Supervision: Gohar Ali, Syed Inayat Ali Shah.

13. Competing Interests

Authors have declared that no competing interests exist.

References

[1] S. Abbasbandy, *Homotopy analysis method for heat radiation equations*, International Communications in Heat and Mass Transfer **34**, (2007) 380 - 387.

[2] S. Abbasbandy and A. Shirzadi, *A new application of the homotopy analysis method: Solving the Sturm-Liouville problems*, Commun Nonlinear Sci Numer Simulat **16**, (2010) 112-126.

[3] K. A. Abro and M. A. Solangi, *Heat Transfer in Magnetohydrodynamic Second Grade Fluid with Porous Impacts using Caputo-Fabrizoi Fractional Derivatives*, Punjab Univ. j. math. **49**, No. 2 (2017) 113-125.

[4] N. Acharya, K. Das and P. K. Kundu, *The squeezing flow of Cu-water and Cu-kerosene nanofluids between two parallel plates*, Alexandria Engineering Journal **55**, (2016) 1177-1188.

[5] A. Ali, M. Tahir, R. Safdar, A. U. Awan, M. Imran and M. Javaid, *Magnetohydrodynamic Oscillating and Rotating Flows of Maxwell Electrically Conducting Fluids in a Porous Plane*, Punjab Univ. j. math. **50**, No. 4 (2018) 61-71.

[6] F. Ali, I. Khan, S. U. Haq and S. Shafie, *Influence of Thermal Radiation on Unsteady Free Convection MHD Flow of Brinkman Type Fluid in a Porous Medium with Newtonian Heating*, Mathematical Problems in Engineering **2013**, (2013), doi.org/10.1155/2013/632394.

[7] A. Alsaedi, M. I. Khan, M. Farooq, N. Gull and T. Hayat, *Magnetohydrodynamic (MHD) stratified bioconvective flow of nanofluid due to gyrotactic microorganisms*, Advanced Powder Technology **28**, (2017) 288 - 298.

[8] H. A. Attia and N. A. Kotb, *MHD flow Between Parallel Plates with Heat transfer*, Acta Mechanica **117**, (1996) 215 - 220.

[9] B. Bin-Mohsin, N. Ahmed, U. Adnan Khan and S. T. Mohyud-Din, *A bioconvection model for a squeezing flow of nanofluid between parallel plates in the presence of gyrotactic microorganisms*, Eur. Phys. J. Plus **132**, (2017) 187.

[10] A. K. Borkakoti and A. Bharali, *Hydromagnetic flow and heat transfer between two horizontal plates*, The lower plate being a stretching sheet. Q. Apple. Math. **41**, (1983) 461 - 467.

[11] A. J. Chamkha and A. B. Nakhi, *MHD mixed convection-radiation interaction along a permeable surface immersed in a porous medium in the presence of Soret and Dufour's effects*, Heat Mass Transf. **44**, (2008) 845 - 856.

[12] S. H. Chatraei, C. W. Macosko and H. H. Winter, *Lubricated squeezing flow: A new biaxial extensional Rheometer*, J. Rheol. **25**, (1981) 433-443.

[13] U. S.Choi, *Thermal Conductivity of Fluids with Nanoparticles*, Developments and Application of Non-Newtonian Flows. ASME **66**, (1995) 99-105.
[14] S. U. S. Choi, *Nanofluids from vision to reality through research*, Journal of Heat Transfer **131**, (2009) 1-9.
[15] S. U. S. Choi, Z. G. Zhang, P. Keblinski and H. S. Nalwa, *Nanofluids Encyclopedia of Nanoscience and Nanotechnology*, Los Angeles, Calif, USA American Scientific **6**, (2004) 737 - 757.
[16] S. K. Das, S. U. S. Choi and H. E. Patel, *Heat transfer in nanofluids-A review*, Heat Transfer Engineering **27**, (2006) 3 -19.
[17] H. M. Duwairi, B. Tashtoush and R. A. Damseh, *On heat transfer effects of a viscous fluid squeezed and extruded between two parallel plates*, Heat Mass Transf **41**, (2004) 112.
[18] M. A. A. Hamad, *Analytical solution of natural convection flow of a nanofluid over a linearly stretching sheet in the presence of magnetic field*, International Communications in Heat and Mass Transfer **38**, (2011) 487-492.
[19] S. Goodman, *Radiant-heat transfer between non gray parallel plates*, Journal of Research of the National Bureau of Standards **58**, (1957) Research Paper 2732.
[20] T. Hayat, T. Abbas, M. Ayub, T. Muhammad and A. Alsaedi, *On Squeezed Flow of Jeffrey Nanofluid between Two Parallel Disks*, Appl. Sci. **6**, (2016) 346.
[21] T. Hayat, A. Qayyum, F. Alsaadi, M. Awais, M. Abdullah and M. A. Dobaie, *Thermal radiation effects in squeezing flow of a Jeffery fluid*, Eur. Phys. J. Plus **128**, (2013) 85.
[22] T. Hayat, A. Yousaf, M. Mustafa and S. Asghar, *Influence of heat transfer in the squeezing Flow between paralleld disks*, Chemical Engineering Communications **199**, No. 8 (2012) 1044 - 1062.
[23] A. Hussain, S. T. Mohyud-Din and T. A. Cheema, *Analytical and numerical approaches to squeezing flow and heat transfer between two parallel disks with velocity slip and temperature jump*, Chin. Phys. Lett. **29**, No. 11 (2012) 1147705.
[24] S. A. Hussain, S. Muhammad, G. Ali, S. I. A. Shah, M. Ishaq, Z. Shah, H. Khan, M. Tahir and M. Naeem, *A Bioconvection Model for Squeezing Flow between Parallel Plates Containing Gyrotactic Microorganisms with Impact of Thermal Radiation and Heat Generation/Absorptio*, Journal of Advances in Mathematics and Computer Science **27**, No. 4 (2018) 1-22.
[25] M. Ishaq, G. ali, S. I. A. Shah, Z. Shah, S. Muhammad and S. A. Hussain, *Nanofluid Film Flow of Eyring Powell Fluid with Magneto hydrodynamic effect on Unsteady Porous Stretching Sheet*, Punjab Univ. j. math. **51**, No. 3 (2019) 147-169.
[26] W. A. Khan, O. D. Makinde and Z. H. Khan, *The MHD boundary layer flow of a nanofluid containing gyrotactic micro-organisms past a vertical plate with Navier slip*, Int. J. Heat Mass Transf **74**, (2014) 285 -291.
[27] W. A. Khan and O. D. Makinde, *MHD nano fluid bioconvection due to gyrotactic micro-organisms over a convective heat stretching sheet*, International Journal of Thermal Sciences **81**, (2014) 118 - 124.
[28] H. Khan, M. Hanif, Z. Shah, S. Islam, W. Khan and S. Muhammad, *The Combined Magneto Hydrodynamic and Electric Field Effect on an Unsteady Maxwell Nanofluid Flow over a Stretching Surface under the Influence of Variable Heat and Thermal Radiation*, Appl. Sci.2 **8**, (2018) doi: 10.3390/app8020160.
[29] U. Khan, N. Ahmed and S. T. Mohy-ud-Din, *Analysis of magnetohydrodynamic flow and heat transfer of Cu-water nanofluid between parallel plates for different shapes of nanoparticles*, Neural Comput. Appl. **29**, (2018) 695-703.
[30] U. Khan, N. Ahmed, S. T. Mohy-ud-Din and B. Bin-Mohsin, *A bioconvection model for MHD flow and heat transfer over a porous wedge containg both nanoparticles and gyrotatic microorganisms*, Biol. Syst. J. **24**, (2016) 409.
[31] A. V. Kuznetsov and D. A. Nield, *The Cheng-Minkowycz problem for natural convective boundary layer flow in a porous medium saturated by a nanofluid: A revised model*, Int. J. Heat Mass Transf **65**, (2013) 682 - 685.
[32] S. J. Liao, *The proposed homotopy analysis method for the solution of nonlinear problems*, PhD Thesis. Shangai Jiao Tong University, 1992.
[33] S. J. Liao, An explicit totally analytic approximate solution for blasius viscous flow problems, Int. J. Non-linear Mech. **34**, (1999) 759 - 778.
[34] S. J. Liao, *On the Analytic Solution of Magnetohydrodynamic Flows of Non-Newtonian Fluids over a Stretching Sheet*, J. Fluid Mech. **488**, (2003) 189 - 212.

[35] S. J. Liao, *On Homotopy Analysis Method for Nonlinear Problems*, Appl. Math .Comput. **147**, (2004) 499-513.

[36] S. J. Liao, *An Analytic Solution of Unsteady Boundary Layer Flows Caused by Impulsively Stretching Plate*, Commun. Nonlinear Sci. Numer. Simul. **11**, (2006) 326 - 339.

[37] S. J. Liao, An optimal homotopy-analysis approach for strongly nonlinear differential equations, Commun. Nonlinear Sci. Numer. Simul. **15**, (2010) 2003 - 2016.

[38] M. Mahmoodi, S. H. Kandelousi, Kerosene?alumina nanofluid flow and heat transfer for cooling application, J. Cent. South Univ **23**, (2016) 983 - 990.

[39] H. Masuda, A. Ebata, K. Teramae and N. Hishinuma, *Alteration of Thermal Conductivity and Viscosity of Liquid by Dispersing Ultra-Fine Particles*, Netsu Bussei. **7**, No. 4 (1993) 227-233.

[40] S. Muhammad, G. Ali, Z. Shah, S. Islam and S. A. Hussain, *The Rotating Flow of Magneto Hydrodynamic Carbon Nanotubes over a Stretching Sheet with the Impact of Non-Linear Thermal Radiation and Heat Generation/Absorption*, Appl. Sci. **8**, (2018) doi:10.3390/app8040000.

[41] S. Muhammad, S. I. A. Shah, G. Ali, M. Ishaq, S. A. Hussain and H. Ullah, *Squeezing Nanofluid Flow Between Two Parallel Plates Under The Influence Of MHD and Thermal Radiation*, Asian Research Journal of Mathematics **10**, No. 1 (2018) 1-20, 2018.

[42] M. Mustafa, T. Hayat and S. Obaidat, *On heat and mass transfer in the unsteady squeezing flow between parallel plates*, Meccanica **47**, (2012) 1581.

[43] T. J. Pedley, N. A. Hill and J. O. Kessler, *The growth of bioconvection patterns in a uniform suspension of gyrotactic micro-organisms*, J. Fluid Mech. **195**, (1988) 223 - 237.

[44] A. Raees, H. Xu and S. Liao, *Effects of Viscous Dissipation on Unsteady MHD Thermo Bioconvection Boundary Layer Flow of a Nanofluid Containing Gyrotactic Microorganisms along a Stretching Sheet*, Int. J. Heat Mass Transfer **86**, (2015) 174.

[45] M. M. Rashidi, H. Shahmohamadi and S. Dinarvand, *A Series Solution for Three-Dimensional Navier - Stokes Equations of Flow near an Infinite Rotating Disk*, Math. Prob. Eng. (2008) 935095.

[46] R. Safdar, M. Imran, M. Tahir, N. Sadiq and M. A. Imran, *MHD Flow of Burgers' Fluid under the Effect of Pressure Gradient Through a Porous Material Pipe*, Punjab Univ. j. math. **50**, No. 4 (2018) 73-90.

[47] M. Sheikholeslami and D. D. Ganji, *Three dimensional heat and mass transfer in a rotating system using nanofluid*, Powder Technol **253**, (2014) 789 - 796.

[48] M. Sheikholeslami, M. Hatami and D. D. Ganji, *Nanofluid flow and heat transfer in a rotating system in the pre sence of a magnetic field*, J. of Molecular Liquids **190**, (2014) 112 - 120.

[49] P. Singh, V. Radhakrishnan and K. A. Narayan, *Squeezing flow between parallel Plates Ingenieur*, Archiv. **60**, (1990) 274-281.

[50] D. Srinivasacharya, B. Mallikarjuna and R. Bhuvanavijaya, *Soret and Dufour effects on mixed convection along a vertical wavy surface in a porous medium with variable properties*, Ain Shams Engineering **6**, (2015) 553 - 564.

[51] M. J. Stefan, *Versuch Uber die scheinbare adhesion, Sitzungsberichte der Akademie der Wissenschaften in Wien*, Mathematik-Naturwissen **69**, (1874) 713-721.

[52] R. L. Verma, *A numerical solution to squeezing flow between parallel channels*, Wear **72**, (1981) 89-95.

[53] W. Yu, D. M. France, J. L. Robert and S. U. S. Choi, *Review and comparison of nanofluid thermal conductivity and heat transfer enhancement*, Heat Transfer Engineering **29**, (2008) 432- 446.

[54] A. A. Zafar, M. B. Riaz and M. A. Imran, *Unsteady Rotational Flow of Fractional Maxwell Fluid in a Cylinder Subject to Shear Stress on the Boundary*, Punjab Univ. j. math. **50**, No. 2 (2018) 21-32.